Comparative investigation of two-dimensional imaging methods and X-ray tomography in the characterization of microstructure

Inigo Bacaicoa, Martin Lütje, Philipp Sälzer, Cristin Umbach, Angelika Brückner-Foit, Hans-Peter Heim and Bernhard Middendorf, Kassel, Germany

Article Information

Correspondence Address
Dipl.-Ing. Philipp Sälzer
Abteilung Materialentwicklung und Verbundwerkstoffe
Institut für Werkstofftechnik, Kunststofftechnik
Universität Kassel
34125 Kassel, Germany
E-mail: saelzer@uni-kassel.de

Keywords
X-ray tomography, micrographs, dynamic image analysis, Al-Si-Cu-alloys, wood-plastic composites (WPC), foam concrete

The microstructural features of three different materials have been quantified by means of 2D image analysis and X-ray micro-computer tomography (CT) and the results were compared to determine the reliability of the 2D analysis in the material characterization. The 3D quantification of shrinkage pores and Fe-rich inclusions of an Al-Si-Cu alloy by X-ray tomography was compared with the statistical analysis of the 2D metallographic pictures and a significant difference in the results was found due to the complex morphology of shrinkage pores and Fe-rich particles. Furthermore, wood particles of a wood-plastic composite were measured by dynamic image analysis and X-ray tomography. Similar results were obtained for the maximum length of the particles, although the results of width differ considerably, which leads to a miscalculation of the particles aspect ratio. Finally, air voids of a foam concrete were investigated by the analysis of the 2D pictures in ImageJ and the results of the 2D circularity were compared with the values of the 3D elongation obtained by micro-computed tomography. The 3D analysis of the air voids in the foam concrete showed a more precise description of the morphology, although the 2D result are in good agreement with the results obtained by X-ray micro-tomography.

The use of X-ray computer tomography is increasingly becoming a widespread tool in materials science since the 3D image acquisition provides new insights into material optimization, damage analysis and microstructural modeling. The application of X-ray tomography in the microstructural analysis requires the development of volumetric quantification methods to determine the morphological and quantitative parameters that best characterize the microstructure. Material characterization and process optimization investigations have been based on the analysis of 2D micrographs as they are a useful method to quantify the relevant material features. However, given the morphological complexity of the microstructural elements, the accuracy of these results may be questioned. On the other hand, computed tomography enables a better understanding of the microstructural morphology generated in different production processes and their influence on the fracture behavior of materials.

In this study, the 3D quantification of the microstructural features related to the damage mechanism are analyzed by X-ray tomography in different materials and compared with the results from the corresponding 2D image analysis.

First of all, cast Al-Si-Cu alloys are essential in the automotive industry due to their excellent mechanical properties, castability and recycling possibilities. The application of these alloys as structural components requires the characterization of the casting defects since they can lead to rapid failure when certain amount of cycling loading is applied. Casting pores have been reported to act as main crack initiation sites above a critical size [1, 2] and hard intermetallic particles such as Fe-rich particles can also promote crack initiation if they are large compared to pores [3, 4]. Several investigations have reported the high morphological complexity of these defects and their tendency to form large clusters, which has a decisive influence on the damage process [5, 6].

Wood-plastic composites (WPC) gained significance as a commercial material in the last twenty years. Besides the building and construction industries, these materials are applied more and more in technically oriented industries and are usually processed by extrusion or injection molding [7, 8]. To improve reliability of such composites, the processed wood fillers need to be characterized as their size and shape have a significant influence on the mechanical properties [9]. Most of the previous research, dealing with the influence of particle size on the mechanical properties, used two-dimensional methods to characterize such features [10-13]. Some investigations show a huge influence of the aspect ratio of the particle [14-16]. It is to be expected that especially the results of shape, e. g., aspect ratio, of particles are depending on the type of measurement and therefore differ between two-dimensional image analysis and three-dimensional X-ray tomography. Furthermore, the orientation within the sample is an important factor, which can be better characterized by a three-dimensional method like X-ray tomography [17, 18]. Additionally, such measurements are suitable to qualify internal damages like cracks and delamination [19].

In the ongoing research of ultra-high performance concrete (UHPC) [20], a high strength mineral foam was developed at TU Dortmund University [21]. The development was continued at the University of Kassel [22]. Today, air curing foams with densities between 0.5 to 1.3 kg × dm^{-3} and a compressive strength of 2.5 to 18.0 MPa can be fabricated with different mix designs. In a current research project, multifunctional mineral wall elements made of mineral foam in combination with UHPC shells are being developed for the manufacturing of urban housing prefabricated modular parts. The combination of high-performance materials such as UHPC and mineral foams enables the optimization of strength and structural tightness as well as the liquid penetration resistance and thermal insulation.

Materials and experiments

Al-Si-Cu alloy. Table 1 shows the chemical composition of the studied near-to-eutectic Al-Si-Cu alloy. The iron content is 0.6 wt.-% which forms a considerable amount of β-Al_5FeSi phases together with the less detrimental α-$Al_{15}(Fe,Mn)_3Si_2$.

The material was sand casted in 4 mm thick sheets in a sodium silicate mold at room temperature and 20 mm long specimens were machined out with a square cross section of 4 × 4 mm^2 for the CT analysis.

The metallographic samples were examined by optical microscopy and scanning electron microscopy after following standard metallographic procedures in the preparation of the specimens. Color contrast and shape filters were applied to differentiate the β-phase from the rest of the material. ImageJ was used as an image analysis software for the quantitative metallography with a minimum of 60 images at 200× magnification per specimen to generate data regarding length of the β-Al_5FeSi inclusions.

The three-dimensional measurements were carried out using a ZEISS Xradia Versa 520 X-ray microscope at a voltage of 60 kV and a current of 85.6 µA in the analysis of the Fe-rich inclusions, after which 995 radiographs were captured with a resolution of 1.0 µm and an exposure time of 12 s. For the shrinkage pores, 1601 records have been taken with an exposure time of 12 s, 40 kV and 3 W source power. A low energy filter was applied to the source and the voxel size was 2.3 µm. The raw data was reconstructed with a pixel center shift of 0.25 and a standard beam hardening coefficient of 0.7.

After image correction with filters, the acquired radiographs were reconstructed with "TXM Reconstructor" (ZEISS) software. The image analysis was carried out with the commercial rendering package Avizo, in which the β-Al_5FeSi inclusions were manually segmented and the shrinkage pores and gas pores were segmented using a grayscale thresholding tool. After applying the non-local means filter, data of volume, surface and size of each inclusion were obtained.

Wood-plastic composites. The investigated plastic material is a polypropylene obtained by Sabic (Saudi Basic Industries Corporation, Saudi Arabia), compounded with 10 wt.-% of the wood filler Arbocel C 320 by JRS (J. Rettenmaier & Söhne GmbH & Co. KG, Germany). After compounding the raw materials, test specimens of type 1a were made according to DIN EN ISO 527 using an injection molding machine. The initial particle size is influenced by the two processing steps compounding and injection molding which results in a significant shortening of the particle size.

A dynamic image analysis (DIA) was carried out to characterize the remaining particle size after processing. Unlike X-ray micro-tomography, the particles have to be separated by the matrix polymer to be measured with a DIA. This was realized using a simplified Soxhlet extraction. About 10 g of the sample was inserted in boiling xylene for 5 h to dissolve the polymer material. The dynamic image analysis system Qicpic (Sympatec GmbH, Germany) uses a high-speed camera to capture images of the particles, which are dispersed inside a liquid. The camera captures images with 4.2 MP at 175 Hz. With an optical magnification of 1.3, the resulting pixel size is 4.2 µm. The measurement time amounts 60 s.

To characterize the particle size, the maximum and minimum Feret diameter were evaluated to gain information about particle length and width. Furthermore, the aspect ratio, which is defined as the ratio of minimum to maximum Feret diameter, was calculated to characterize particle shape. To reduce the measurement inaccuracy and increase the comparability of both methods, only particles longer than 100 µm were taken into consideration for the evaluation. Especially very small particles with the size of just one pixel could distort the results, providing an ideal aspect ratio of 1, because of the same length and width.

The comparative three-dimensional measurements were carried out using a Zeiss Xradia Versa 520 at a voltage of 50 kV and a current of 79 µA. 1601 images were captured with a resolution of 4.8 µm and an exposure time of 4 s for each image. Afterwards, the images have been reconstructed using the Zeiss TXM Reconstructor software. The image analysis was made by using the software Avizo (FEI). After applying a non-local means filter, an automatic segmentation of wood particles was carried out using a greyscale thresholding. The length of the particles was evaluated using the parameter Length3d of the Label Analysis option, which equals the maximum Feret diameter in a three-dimensional orientation. Comparing to the two-dimensional measurements, the width of particles was evaluated using the parameter

Si	Cu	Mg	Fe	Zn	Mn	Ni	Ti	Al
12.96	1.52	0.68	0.6	0.48	0.17	0.05	0.04	Balance

Table 1: Chemical composition of the Al-Si-Cu alloy (wt.-%)

Width3d, which corresponds to the minimum Feret diameter. The aspect ratio was calculated in the same way as it is described above and is therefore given by the ratio of Width3d to Length3d. As in the dynamic image analysis only particles longer 100 µm were taken into consideration for the evaluation to keep the results comparable to each other.

Foam concrete. The foam concrete used is based on a five component UHPC mortar. To decrease the bulk density, quartz sand and quartz powder are replaced by the lightweight aggregate perlite in different particle sizes. Fine basalt fibers and dispersible polymer powder based on an ethylene vinyl acetate copolymer are used to stabilize the mixture. With a water to binder ratio of 0.34, a very flowable concrete was fabricated. For the foaming process, an aluminum paste based on the solvent diethylene glycol with an average particle size of 12 µm was used. The resulting density was 0.5 kg × dm^{-3} with a total porosity of 61 % and a compressive strength of 2.5 MPa.

The 2D air void analysis is limited by the resolution of the applied optics. In case of foamed concrete, a digital reflex camera was used to get sufficient data for meaningful results. The concrete surface has to be smooth and illuminated by light coming from sideways. The images were analyzed using the computer program "ImageJ". For this purpose, the pores were selected and ellipses with the same maximal diameter were adjusted. These ellipses and the selected data itself were analyzed and different parameters were calculated. These included the shape parameters pore area and circularity. For comparison, 3D measurements were done using a Zeiss Xradia Versa 520. At a voltage of 140 kV and a current of 71.2 µA, 1601 radiographs were captured with a resolution of 26.8 µm and an exposure time of 2 s for each image. The reconstruction was carried out by the Zeiss software TXM Reconstructor and the further analysis was made using Avizo 9.2 (FEI). After applying filter corrections, the data was segmented with the threshold method in the segmentation editor of the software. The evaluation was done using the 3D shape parameters 3D volume and elongation.

Results and discussion

Al-Si-Cu alloy. Long needle-like β-phases were found in the 2D micrographs with an average length of 146 µm and an area fraction of 6.5 %. The eutectic Si particles are present in form of long needles and it can be observed that some Al_2Cu particles lie along the β-Al_5FeSi inclusions (see Figure 1).

The 3D reconstructions of these particles (see Figure 2) reveal their plate-like morphology with an average volume of 0.0018 mm^3, surface area of 0.358 mm^2 and maximum Feret size of 347 µm. Figure 3 shows the distributions of the maximal Feret size from the 2D and 3D analysis in which a significant difference can be noted. This indicates that the 2D analysis leads to an underestimation of the average and maximum length of the β-Al_5FeSi particles as well as the upper tail of the distribution.

As it can be observed in Figure 4, these inclusions tend to agglomerate to large clusters, some of which seem to be arranged perpendicular to a certain axis. This agglomeration of inclusions causes the joint of particles by branching or even crossing leading to more complex particles rather than simple plates (see Figure 5). These complexities are the reason why stereological relations are not applicable in the conversion of size distribution from 2D to 3D and the quantifications of β-Al_5FeSi inclusions based on 2D analyses require the use of safety factors for the fracture mechanical assessment.

Moreover, β-Al_5FeSi compounds tend to form cavities in which micro-pores are enclosed what can be seen in Figure 6. This suggests that the β-phase platelets may enhance the formation of micro-porosity by restricting the flow of the liquid melt dur-

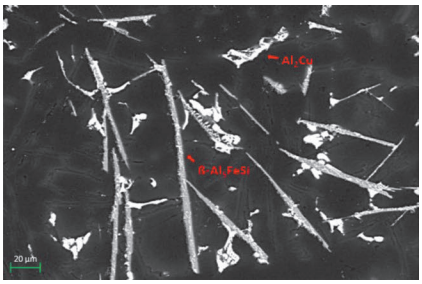

Figure 1: Long needle-like β-Al5FeSi phases with Cu-rich intermetallics

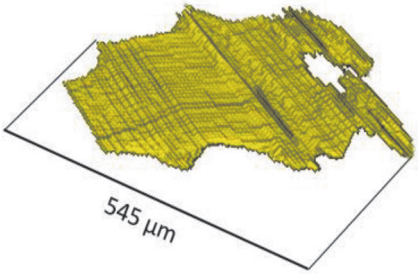

Figure 2: Reconstructed and segmented 3D micro-tomography of a β-Al5FeSi inclusion

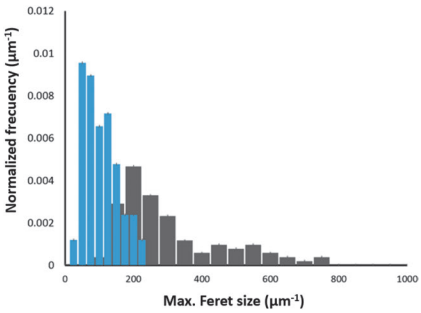

Figure 3: Distribution of the maximum Feret size of the β-Al5FeSi inclusions from the 2D (blue) and 3D (black) quantifications

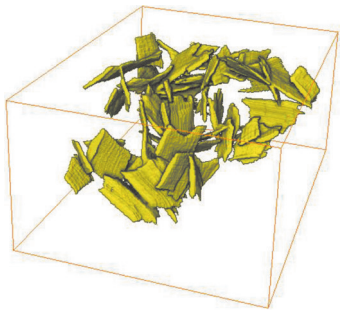

Figure 4: Cluster of β-Al5FeSi phases

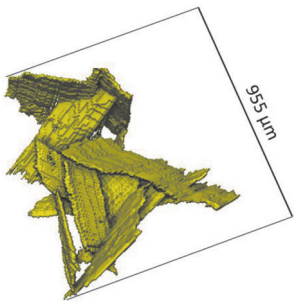

Figure 5: Agglomeration of β-Al5FeSi inclusions

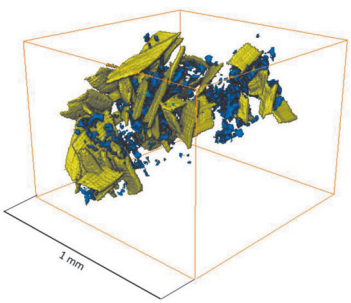

Figure 6: Cluster of β-Al5FeSi particles in which pores are enclosed

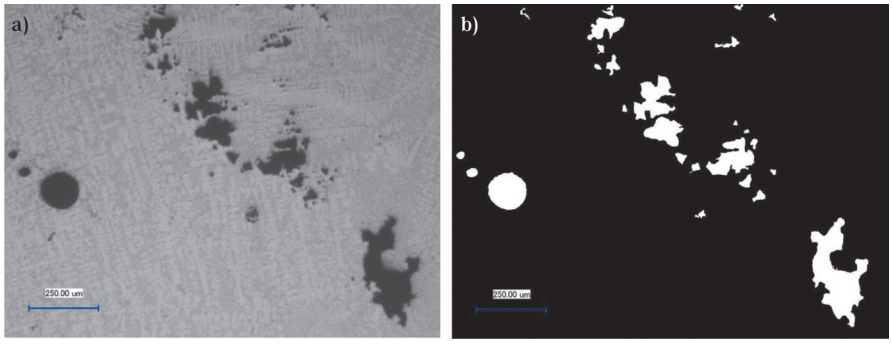

Figure 7: Metallographic images, a) casting pores found in an Al-Si alloy, b) segmented to a binary image

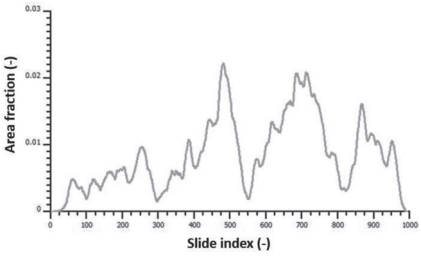

Figure 8: Relationship between slice index and area fraction

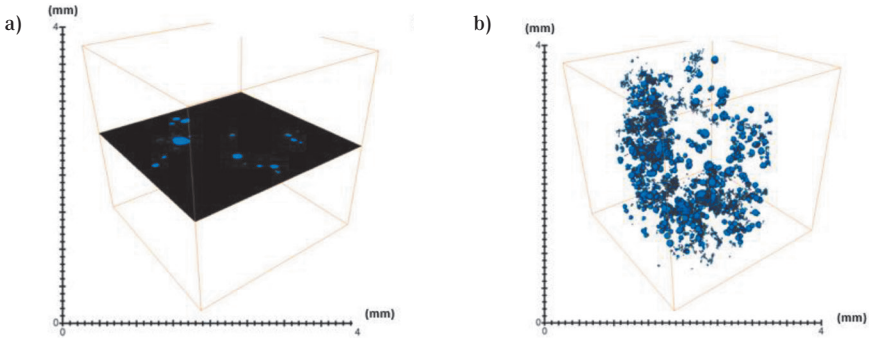

Figure 9: a) Section slice 483 showing maximum area fraction, b) segmented porosity from 3D analysis

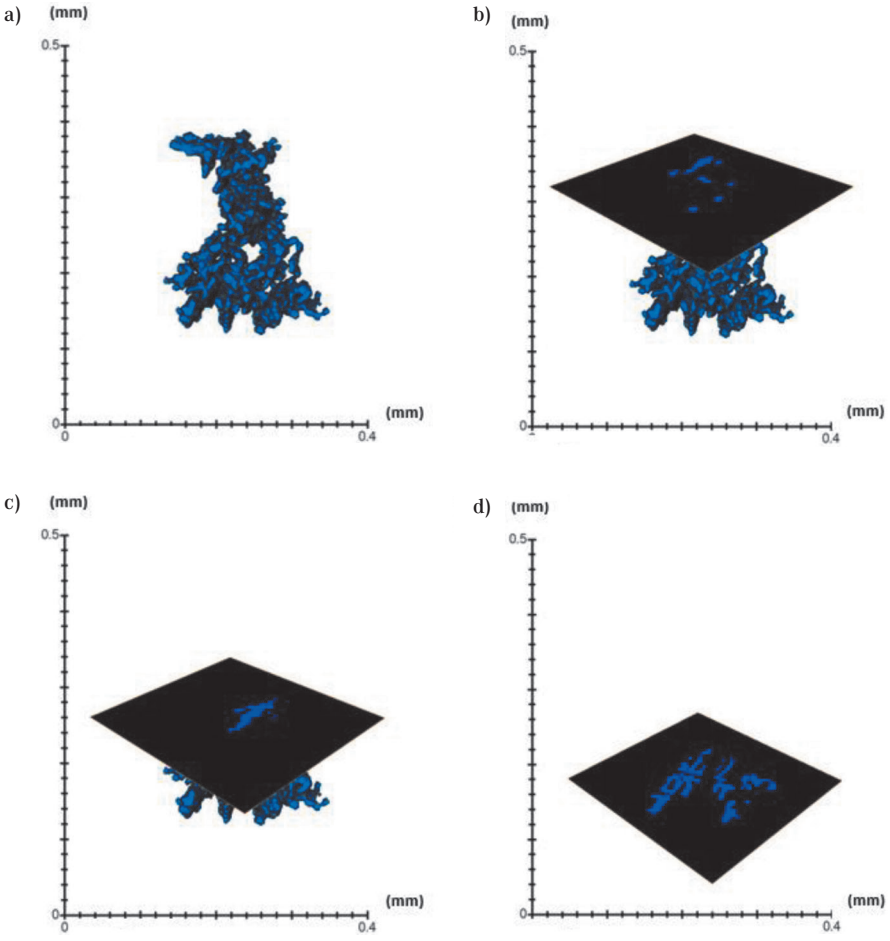

Figure 10: a) Segmented pore, b) pore cut in slice 108, c) pore cut in slice 82, d) pore cut in slice 43

ing the casting. These large clusters of brittle β-Al_5FeSi particles with micro-pores in the vicinity can act as stress concentration raisers and promote rapid crack initiation in the absence of larger pores.

Moreover, large shrinkage pores and gas pores were generated due to the low cooling rate during the casting process in the studied Al-Si-Cu alloy, as it can be observed in Figure 7. The 2D image analyzing technique reveals only a part of the pore structure and can lead to nonconservative results. Figure 7 shows an example of a typical image revealed by optical microscopy with 200× magnification. The image reveals 28 pores with an area fraction of 5.54 %. The defect observation was done for all casting defects in the section, and the area fraction was scaled in relationship to the full section size. This calculation represents an overall area fraction of 1.64 %.

Figure 8 reveals that the area fraction depends on the section of observation. The maximum area fraction for this analysis was 2.2 % in section 483. Figure 9 contains a direct comparison of the 2D and 3D analysis.

A segmented pore (see Figures 10a to 10d) from the 3D data set is cut in slice 108 (see Figure 10b), 82 (see Figure 10c), 43 (see Figure 10d) and shows different results of the area fraction. It is impossible to gain information about the association of the morphology and the porosity. Within an image analysis it would be rather separated as 7 or more porosities when focusing on slice 108 (see Figure 10b) or on the contrary processed as one pore in Figure 10c. To gain information about the complete pore, a 3D analysis of a tomography is needed. The maximum Feret diameter is 291.37 µm and the minimum Feret diameter is 178.06 µm, which have been calculated in 3D. The segmented pore has an area of 0.160 μm^2 and a volume of 0.47 μm^3.

Wood-plastic composites. Typical particles measured with dynamic image analy-

sis and X-ray tomography are shown in Figure 11. Both measurements are based on grey-scale images with a nearly automatic segmentation method.

Plotting the results of particle width on length in a scatter diagram in Figure 12 reveals the difference between both methods. Apparently, the number of particles measured with the dynamic image analysis (124 805 particles) is much higher than using the X-ray micro-tomography (2841 particles). The number of outliers with high particle lengths, which can be seen in the left chart of DIA, is relatively small in relation to the high number of particles. Regarding the particle length, both distributions are comparable. However, the slope of the regression line is very different between both methods, showing a significantly lower width measured by the X-ray tomography.

The evaluated length, width and calculated aspect ratios are given in Table 2. Especially the results of the particle length are nearly identical for both methods. The mean of length is 250 µm measured by X-ray tomography and 254 µm measured by dynamic image analysis, whereas the mean deviation of all length values is below 2 %. Nevertheless, there is a huge difference in the measured particle widths, for which X-ray tomography shows a mean of 65 µm and dynamic image analysis a value of 94 µm, respectively. The deviation between both methods is up to 55 %. This directly affects the calculated aspect ratio. While the values are very similar at the 10th percentile, the results show a significant difference at the 90th percentile.

This difference in aspect ratio becomes obvious in Figure 13, which shows a relative distribution of the calculated aspect ratios for both methods. The distribution measured by the two-dimensional method displays a broad distribution with aspect ratios up to 0.9, which represents nearly cubic shaped particles. However, the three-dimensional measurement shows a significant peak at aspect ratios below 0.3 and nearly no aspect ratios larger than 0.6.

Compared to the other presented two-dimensional methods, the dynamic image analysis does not lack statistical significance, however, it provides an amount of data which is nearly 50 times bigger than the data obtained by X-ray tomography. The dynamic image analysis is also preferred compared to the tomography in terms of measurement duration.

Regarding the quality of the measurement, the presented results show some major differences among the methods. On the one hand, the characterized particle lengths are nearly identical for two- and three-dimensional measurements, but on the other hand the measured widths and therefore the calculated aspect ratios differ from each other.

A closer consideration of the three-dimensional particle shape in Figure 11 shows that the majority of particles is shaped like flat platelets with different sizes in x-, y- and z-direction. The evaluation considers the longest of these direc-

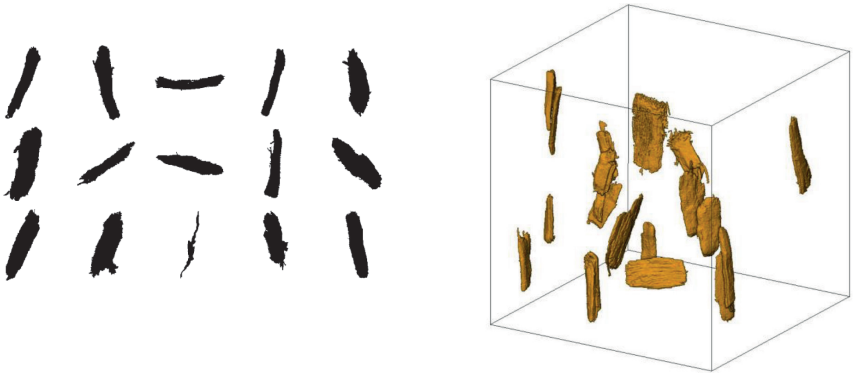

Figure 11: Visualization of particles measured with dynamic image analysis (left) and X-ray tomography (right)

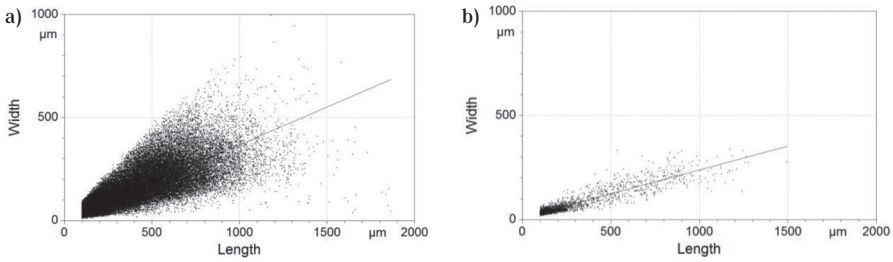

Figure 12: Scatter diagram of particle width over length, a) measured using dynamic image analysis, b) measured using X-ray micro-tomography

	Dynamic image analysis (2D)			X-ray tomography (3D)		
	Length (µm)	Width (µm)	Aspect ratio	Length (µm)	Width (µm)	Aspect ratio
Mean	254	94	0.36	250	65	0.28
10th percentile	105	27	0.21	107	29	0.20
50th percentile	150	57	0.32	159	44	0.27
90th percentile	579	227	0.59	568	146	0.37

Table 2: Results of dynamic image analysis and X-ray tomography

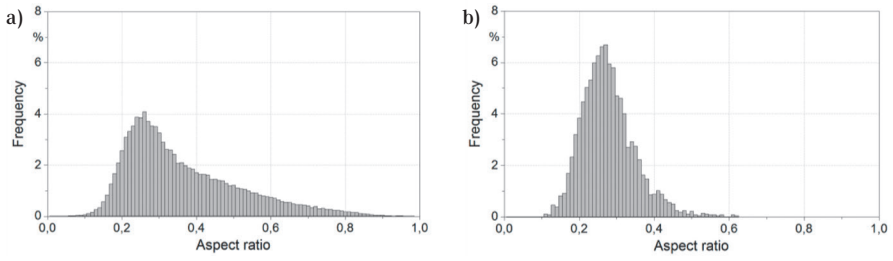

Figure 13: Comparison of calculated aspect ratios between a) dynamic image analysis, b) X-ray tomography

tions as the length and the shortest as the width. The evaluation of particle sizes by dynamic image analysis is based on the two-dimensional projection area of the particle. Due to the liquid dispersion, the particles are oriented nearly parallel to flow direction, enabling a very accurate measuring of particle length. However, the orientation of the other two directions is random, which means the minimal Feret diameter in the projection area is either the width, the thickness or a value between both.

Foam concrete. The two-dimensional analysis contains a 2D area of 4 cm^2 with a data volume of 204 air voids with a lower limit of 0.1 mm^2. The 3D data implied a volume of 8 cm^3 with 2661 air voids. Here, the lower limit was placed by 0.1 mm^3. That means a 2D analysis generates approximately less than 10 % of the data volume of a similar 3D analysis.

The parameters circularity and elongation are both factors to describe the shape. A value of 1.0 means that the shape is round while lower values mean the shape is more elongated. Spherical pores have a good force deflection that results in good mechanical properties. That does not mean in general that elongated pores have a weaker performance, but in this case the stress direction is also important. In Figure 14, the relative frequency of both parameters is illustrated. The 3D data is clearly more distributed while the 2D data has an explicit peak by about 22 % at a circularity of 0.8. Furthermore, the mean value of the 2D data was slightly higher with a value of 0.72. Due to the fact that in the 2D analyses do not take the third axis into account and with less amount of data, the two data sets are not easy to compare.

The correlation between shape and size is shown in Figure 15. Due to the limited data of the 2D analysis, no clear effect could be seen. The wide distribution of the elongation could also be seen, but there is a tendency to lower shape parameters towards larger pore volumes.

The large air voids showed also a greater angle to foaming direction which indicates that these air voids grew together in the foaming process. That led to higher compressive strengths (up to 40 %) when the sample was loaded in foaming direction.

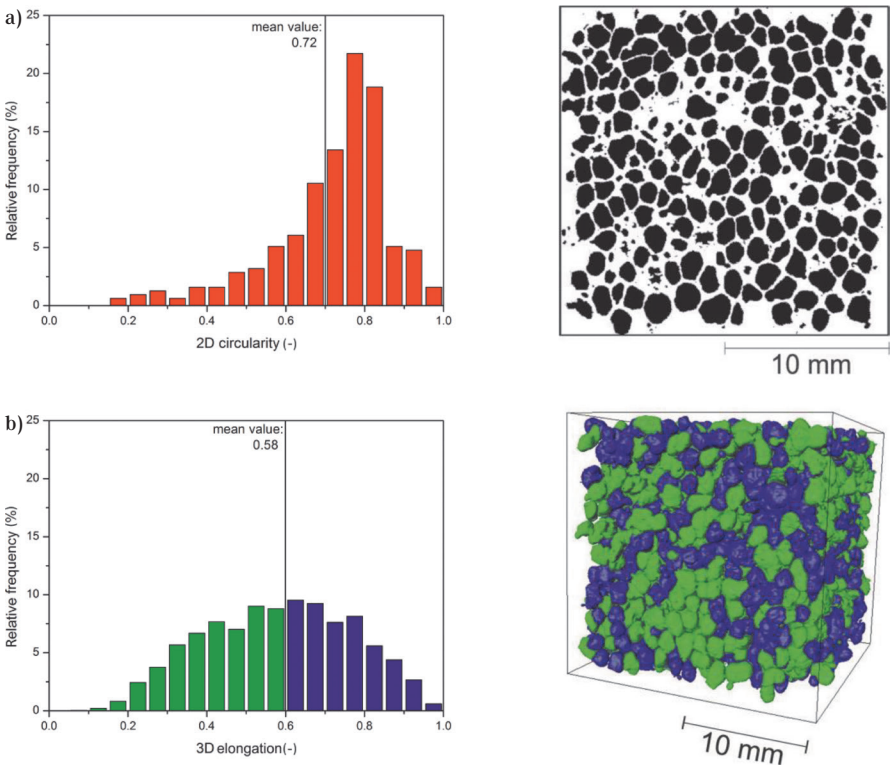

Figure 14: a) Relative frequency of the shape parameters circularity and sphericity, b) model of the pore structure

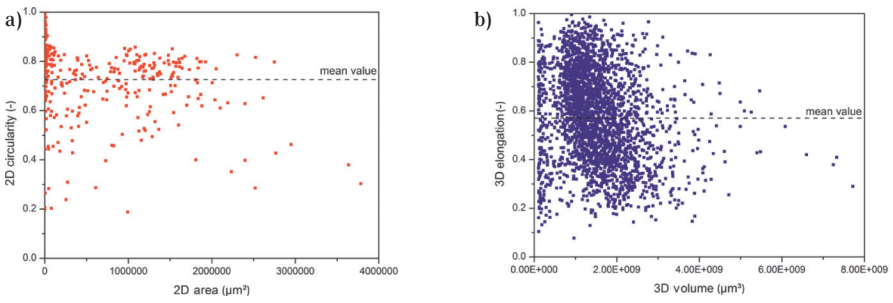

Figure 15: Correlation between shape and size, a) for 2D analysis, b) for 3D analysis

Conclusions

The two-dimensional inspection of materials is a common way to evaluate their properties. For air inclusions in Al-Si-Cu alloys or foam concrete, the 2D analysis depended on the observed area fraction and on the variation of the volume. In case of Al-Si-Cu alloys, the variation depended on the casting process and could be widely spread, especially when big pores occur. In case of foam concrete, the variation depended on the foaming agent, raw materials and rheological properties of the mix design. Moreover, for the macro porous foam concrete, a statistical error occurred due to the smaller amount of data. In wood-plastic composites, the length measurement worked with both methods. The characterization of particle width or even complex shapes using dynamic image analysis (2D method) caused problems, because of the missing third direction. The projection of an area caused a loss of information, producing results that were different from those obtained by X-ray tomography. The same conclusion could be made for β-Al_5FeSi inclusions in Al-Si-Cu alloys and the dispersion of their aspect ratio. A significant difference between the statistical distributions of the 2D and the 3D maximal Feret diameter showed that size and morphology could not be deduced based on stereological relationships.

The missing third dimension made it difficult for all considered materials to analyze complex shapes. A 2D characterization is therefore often not suitable. The more precise 3D analysis is necessary for an accurate assessment of material performance and for material safety.

Acknowledgment

The authors would like to thank the Hessen State Ministry of Higher Education, Research and the Arts – Initiative for the Development of Scientific and Economic Excellence (LOEWE) – for financial support of the special research project "Safer Materials".

References

1 P. D. Lee, T. C. Lindley, C. W. J. Cheong, G. R. Davis, J. C. Elliott: The effect of metallurgical variables and porosity on the high cycle fatigue behaviour of aluminium alloy 319, Proc. of COM2003, in: J. Masounave, G. Dufour (Eds.): host publication, MetSoc, pp. 457-472
2 Q. G. Wang, D. Apelian, D. A. Lados: Fatigue behavior of A356-T6 aluminum cast alloys – Part I: Effect of casting defects, Journal of Light Metals 1 (2001), No. 1, pp. 73-84 DOI:10.1016/S1471-5317(00)00008-0
3 J. Z. Yi, Y. X. Gao, P. D. Lee, T. C. Lindley: Effect of Fe content on fatigue crack initiation and propagation in a cast aluminum-silicon alloy (A356–T6), Materials Science and Engineering A 386 (2004), No. 1-2, pp. 396-407 DOI:10.1016/j.msea.2004.07.044
4 I. Bacaicoa, P. K. Dwivedi, M. Lütje, F. Zeismann, A. Brückner-Foit, A. Geisert, M. Fehlbier: Effect of non-equilibrium heat treatments on microstructure and tensile properties of an Al-Si-Cu alloy, Materials Science and Engineering A 673 (2016), pp. 562-571 DOI:10.1016/j.msea.2016.07.080
5 I. Bacaicoa, M. Lütje, M. Wicke, A. Geisert, F. Zeismann, M. Fehlbier, A. Brückner-Foit: 3D morphology of Al_5FeSi inclusions in high Fe content Al-Si-Cu alloys, Procedia Structural Integrity 2 (2016), pp. 2269-2276 DOI:10.1016/j.prostr.2016.06.284
6 M. Wicke, M. Lütje, I. Bacaicoa, A. Brückner-Foit: Characterization of casting pores in Ferich Al-Si-Cu alloys by microtomography and finite element analysis, Procedia Structural Integrity 2 (2016), pp. 2643-2649 DOI:10.1016/j.prostr.2016.06.330
7 K. Oksman, M. Sain: Introduction, Wood-Polymer Composites, CRC Press, Woodhead Publishing, Boca Raton, Cambridge, UK (2008)
8 M. Feldmann, H.-P. Heim, J.-C. Zarges: Influence of the process parameters on the mechanical properties of engineering biocomposites using a twin-screw extruder, Composites Part A: Applied Science and Manufacturing 83 (2016), pp. 113-119 DOI:10.1016/j.compositesa.2015.03.028
9 C. Clemons: Raw Materials for Wood-Polymer Composites, Wood-Polymer Composites, CRC Press, Woodhead Publishing, Boca Raton, Cambridge, UK (2008), pp. 1-22
10 C. Gozdecki, S. Zajchowski, M. Kociszewski, A. Wilczyński, J. Mirowski: Effect of wood particle size on mechanical properties of industrial wood particle-polyethylene composites, Polimery 56 (2011), No. 5, pp. 375-380
11 A. Nourbakhsh, A. Karegarfard, A. Ashori: Effects of particle size and coupling agent concentration on mechanical properties of particulate-filled polymer composites, Journal of Thermoplastic Composite Materials 23 (2010), No. 2, pp. 169-174 DOI:10.1177/0892705709340962
12 H. Bouafif, A. Koubaa, P. Perré, A. Cloutier: Effects of fiber characteristics on the physical and mechanical properties of wood plastic composites, Composites Part A: Applied Science and Manufacturing 40 (2009), No. 12, pp. 1975-1981 DOI:10.1016/j.compositesa.2009.06.003
13 M. Feldmann: The effects of the injection moulding temperature on the mechanical properties and morphology of polypropylene man-made cellulose fibre composites, Composites Part A: Applied Science and Manufacturing 87 (2016), pp. 146-152 DOI:10.1016/j.compositesa.2016.04.022
14 N. M. Stark, R. E. Rowlands: Effects of wood fiber characteristics on mechanical properties of wood/polypropylene composites, Wood and Fiber Science 35 (2007), No. 2, pp. 167-174
15 C. Gozdecki, A. Wilczyński, M. Kociszewski, S. Zajchowski: Properties of wood–plastic composites made of milled particleboard and polypropylene, European Journal of Wood and Wood Products 73 (2015), No. 1, pp. 87-95 DOI:10.1007/s00107-014-0852-2
16 A. K. Bledzki, O. Faruk: Wood fibre reinforced polypropylene composites: Effect of fibre geometry and coupling agent on physico-mechanical properties, Applied Composite Materials 10 (2003), No. 6, pp. 365-379 DOI:10.1023/A:1025741100628
17 J.-C. Zarges, D. Minkley, M. Feldmann, H.-P. Heim: Fracture toughness of injection molded, man-made cellulose fiber reinforced polypropylene, Composites Part A: Applied Science and Manufacturing 98 (2017), pp. 147-158 DOI:10.1016/j.compositesa.2017.03.022
18 J. Lux, C. Delisée, X. Thibault: 3D characterization of wood based fibrous materials: An application, Image Analysis & Stereology 25 (2006), No. 1, pp. 25-35 DOI:10.5566/ias.v25.p25-35
19 P. J. Schilling, B. R. Karedla, A. K. Tatiparthi, M. A. Verges, P. D. Herrington: X-ray computed microtomography of internal damage in fiber reinforced polymer matrix composites, Composites Science and Technology 65 (2005), No. 14, pp. 2071-2078 DOI:10.1016/j.compscitech.2005.05.014
20 M. Schmidt, E. Fehling, S. Fröhlich, J. Thiemicke: Sustainable Building with Ultra-High Performance Concrete: Results of the German Priority Programme 1182, Kassel, Germany, Kassel University Press, Germany (2014)
21 A. Just: Untersuchungen zur Weiterentwicklung von chemisch aufgetriebenen, lufthärtenden, mineralisch gebundenen Schäumen, Dissertation, TU Dortmund University, Germany (2007)
22 C. Umbach, A. Wetzel, T. Schade, E. Fehling, B. Middendorf: Multifunctional heat-insulating precast UHPC/high strength foam concrete elements for house construction, Proceedings of HiPerMat 2016, 4th International Symposium on Ultra-High Performance Concrete and High Performance Construction Materials, Kassel, Germany (2016)

Bibliography

DOI 10.3139/120.111076
Materials Testing
59 (2017) 10, pages 829-836

ISSN 0025-5300

The authors of this contribution

Inigo Bacaicoa, born in 1991, studied Mechanical Engineering with specialization in Aerospace Engineering at the University of the Basque Country, Bilbao, Spain. During his studies, he worked at ITP, aerospace industry in Zamudio, Spain, in the Department of Materials and Special Processes, analyzing data of micro-cracks and fatigue-loading tests from welding joints for quality assessment. Since 2015, he has been working as a research assistant in the field of casting defects and heat treatment optimization of recycled Al alloys in the Institute of Materials Engineering, Quality and Reliability at the University of Kassel, Germany.

Martin Lütje, born in 1986, studied Mechanical Engineering at the University of Kassel, Germany. After his Master degree, he worked at the Institute of Materials Engineering with the SFB/TRR30 scholarship studying the fatigue behavior of gradient microstructures. Since 2014, he has been working as a research assistant in the field of X-ray tomography and casting defects of Al alloys in the Institute of Materials Engineering, Quality and Reliability at the University of Kassel.

Dipl.-Ing. Philipp Sälzer, born in 1987, studied Mechanical Engineering at the University of Kassel, Germany until 2014 and has been a research assistant in the Department of Polymer Engineering (Prof. Heim) since 2015. Currently, he is working in the field of material development and composite materials in the special research project "Safer Materials" in which he is investigating the influence of the geometry of bio-based fillers.

MSc Cristin Umbach, born in 1989, studied Civil Engineering (Bachelor and Master degree) with scientific specialization in Materials Science and Constructive Engineering at the University of Kassel, Germany. Currently, she is working as a scientific employee in the Institute for Structural Engineering in the Department of Building Materials and Construction Chemistry (Prof. Middendorf) at the University of Kassel.

Prof. Dr. rer. nat. Angelika Brückner-Foit, born in 1953, studied Physics at the University of Karlsruhe, Germany and obtained her PhD in 1980. From 1980 to 1989, she was Head of the Department of Stochastic at the Institute of Materials Research II of Karlsruhe Research Center. From 1985 to 1986, she worked as a guest scientist at the Center for Applied Stochastics Research of Florida Atlantic University, USA. From 1989 to 2000, she was academic supervisor at the Institute of Reliability and Damage in the Mechanical Engineering Department at the University of Karlsruhe. Since 2000, she is Professor in the Department of Quality and Reliability of the Institute of Materials Engineering at the University of Kassel, Germany.

Prof. Dr.-Ing. Hans-Peter Heim, born in 1967, studied Industrial Engineering at the University of Paderborn, Germany. After finishing his PhD, he became chief engineer at the Institute of Plastics Technology at the University of Paderborn in 2001 and has been the acting head of the institute since 2004. Since 2008, he is Professor for Plastics Engineering at the University of Kassel, Germany.

Prof. Dr. rer. nat. Bernhard Middendorf, born in 1962, studied Mineralogy at the University of Cologne, Germany. After his doctorate at the University of Siegen, Germany, he worked as Academic Councilor at the University of Kassel, Germany. Between 2004 and 2012, he worked as Professor in the Department of Building Materials at TU Dortmund University, Germany. Since 2012, he is Professor in the Department of Building Materials and Construction Chemistry at the University of Kassel, Germany.

Abstract

Vergleichsuntersuchung von zweidimensionalen bildgebenden Techniken und Röntgentomographie bei der Charakterisierung von Mikrostruktur. Die mikrostrukturellen Merkmale von drei verschiedenen Werkstoffen wurden mittels 2D-Bildanalyse und Röntgen-Mikrocomputertomographie untersucht und die Ergebnisse verglichen, um die Zuverlässigkeit der 2D-Analyse in der Werkstoffforschung zu bestimmen. Die 3D-Quantifizierung der Schrumpfporen und der eisenhaltigen Einschlüsse einer Al-Si-Cu-Legierung durch Computertomographie wurde mit der statistischen Analyse der zweidimensionalen metallografischen Bilder verglichen. Hierbei ergab sich ein signifikanter Unterschied in den Ergebnissen, der auf die komplexe Morphologie der Poren und Einschlüsse zurückzuführen ist. Weiterhin wurden die Holzpartikel eines Holz-Kunststoff-Verbundes mittels dynamischer Bildanalyse und Mikrocomputertomographie untersucht. Hinsichtlich der Partikellänge konnten mit beiden Methoden sehr ähnliche Ergebnisse erzielt werden. Für die Partikelbreite ergaben sich aufgrund der fehlenden räumlichen Information jedoch deutliche Abweichungen, die zu einer Fehleinschätzung des Partikelseitenverhältnisses führen. Zuletzt wurden die Poren eines Schaumbetons durch Analyse von zweidimensionalen Bildern mittels ImageJ gemessen und die Ergebnisse der Rundheit mit den Werten aus der Computertomographie erhaltenen dreidimensionalen Ausdehnung verglichen. Die 3D-Analyse der Poren im Schaumbeton zeigte eine genauere Beschreibung der Morphologie, obwohl das 2D-Ergebnis in guter Übereinstimmung mit den Ergebnissen der Röntgentomographie steht.